EARTHQUAKE ENGINEERING AND STRUCTURAL DYNAMICS, VOL. 25, 357–369 (1996)

THREE-DIMENSIONAL DYNAMIC RESPONSE OF LINED TUNNELS DUE TO INCIDENT SEISMIC WAVES

I. D. MOORE AND F. GUAN

Geotechnical Research Centre, Faculty of Engineering Science, The University of Western Ontario, London, Ont. Canada N6A 5B9

SUMMARY

Formulae are developed to determine the three-dimensional response of twin lined tunnels buried in an infinite medium subjected to seismic loadings using the method of successive reflection. The convergence of the method has been demonstrated both analytically and numerically. The dynamic interaction of the twin tunnels subjected to seismic waves is investigated numerically. It is found that the three-dimensional response of twin tunnels may differ significantly from the two-dimensional response, and that through-soil interaction between the tunnels may also be significant.

KEY WORDS: three-dimensional; multiple successive reflections; seismic waves; tunnels

INTRODUCTION

The assessment of buried pipelines and subway tunnels for structural stability during earthquakes is important when those structures can potentially be subjected to seismic ground motion. Observations in the field and previous numerical studies have shown that amplification of seismic motions and stress concentrations may occur as a result of wave scattering around such structures.

Pao and Mow[1] were the first to study wave diffraction around a cylindrical cavity in an infinite medium and the resulting stress concentration using wave function expansions. An analytic model was presented by Trifunac[2] to study horizontal polarized shear (SH) wave scattering at a semi-cylinder located at the boundary of a half-space, and Wong and Trifunac[3] investigated analytically SH wave scattering at a semi-elliptic cylinder. SH wave scattering for various topographies has also been studied by Wong and Jennings[4] and by Dravinski[5] using the boundary element method (BEM). The study of vertically polarized (SV), plane longitudinal (P) and Rayleigh wave motions was examined by Wong[6] by means of the solutions of buried line pressure and shear sources. The seismic response of a lined tunnel under incident SH wave in a half-space was investigated by Lee and Trifunac[7] by studying twin tunnels in a full-space using the co-ordinate transform technique. Balendra *et al.*[8] used the same technique to study the SH response of two tunnels in a half-space. Okumaua *et al.*[9] studied the two-dimensional seismic response of twin tunnels by the finite element method. Datta and others have undertaken a systematic study on wave scattering around single or multiple cavities (Wong *et al.*[10] used a hybrid finite element method and wave function expansions to study scattering at an inclusion; Shah *et al.*[11] presented two-dimensional results for wave scattering by multiple scatterers; Chin *et al.*[12] and Liu *et al.*[13] studied the response of pipelines buried in back-filled trenches).

In reality, many underground structures are constructed in close proximity and the interaction between such closely spaced structures may be significant.[9,14] The purpose of this paper is to investigate the three-dimensional response of a pair of lined cylindrical cavities located in a full-space subjected to incident seismic waves. The method of successive reflections (MSR) is employed,[15,16] where the twin lined tunnels are uncoupled and analysed independently. The interaction between them is determined by transforming co-ordinate systems for the wave function expansions.

The work contains a brief review of the theoretical analysis. This is followed by a parametric study of the twin tunnel problem.

CCC 0098–8847/96/040357–13

Received 8 June 1993
Revised 31 October 1995

SOLUTION TECHNIQUE

Solution of the equations of motion

The geometry of the problem is as shown in Figure 1. The parallel twin tunnels, denoted I and II, are deeply buried in a viscoelastic ground material described by the shear modulus μ, mass density ρ and Poisson's ratio σ. The material propeties for the linings are described by μ_{I}, ρ_{I}, σ_{I} and μ_{II}, ρ_{II}, σ_{II} repectively. For convenience, the index indicating the media or the tunnel linings is omitted in equations (1)–(4), which are valid for each of these three different materials.

The displacements and stresses in these solids can be expressed in terms of potentials ϕ, φ and χ, which satisfy the following wave equations of motion:

$$\nabla^2\phi - k_\alpha^2\,\phi = 0 \tag{1a}$$

$$\nabla^2(\varphi,\chi) - k_\beta^2(\varphi,\chi) = 0 \tag{1b}$$

$$k_\alpha = \frac{\omega}{v_{\mathrm{L}}}, \quad k_\beta = \frac{\omega}{v_{\mathrm{T}}} \tag{1c}$$

where ω is the excitation frequency, v_{L} and v_{T} denote longitudinal and transverse wave velocities and

$$\nabla^2 = \frac{1}{r}\frac{\partial}{\partial r}\left(r\frac{\partial}{\partial r}\right) + \frac{1}{r^2}\frac{\partial^2}{\partial\theta^2} + \frac{\partial^2}{\partial z^2} \tag{2}$$

It is understood that the factor $\mathrm{e}^{-i\omega t}$ is omitted in the text.

The general solution of equation (1) takes the following form:

$$\sum_{n=0}^{\infty}(\phi_n,\varphi_n,\chi_n) = \sum_{n=0}^{\infty} H_n(\alpha_v r)\begin{Bmatrix}\cos n\theta\\ \sin n\theta\end{Bmatrix}\left(\begin{Bmatrix}A\\ B\end{Bmatrix}_n \mathrm{e}^{\pm i\gamma_{\mathrm{L}}z}, \begin{Bmatrix}C\\ D\end{Bmatrix}_n \mathrm{e}^{\pm i\gamma_{\mathrm{T}}z}, \begin{Bmatrix}E\\ F\end{Bmatrix}_n \mathrm{e}^{\pm i\gamma_{\mathrm{T}}z}\right) \tag{3}$$

where H_n are the Bessel functions that satisfy the radiation conditions. Bessel functions of the first kind are used for the liners, and the outgoing wave in the medium is expressed in terms of Hankel functions of the first kind. The wave numbers α_v (v = L, T) are given by

$$\alpha_{\mathrm{L}} = \sqrt{\omega^2/v_{\mathrm{L}}^2 - \gamma_{\mathrm{L}}^2} \tag{4a}$$

$$\alpha_{\mathrm{T}} = \sqrt{\omega^2/v_{\mathrm{T}}^2 - \gamma_{\mathrm{T}}^2} \tag{4b}$$

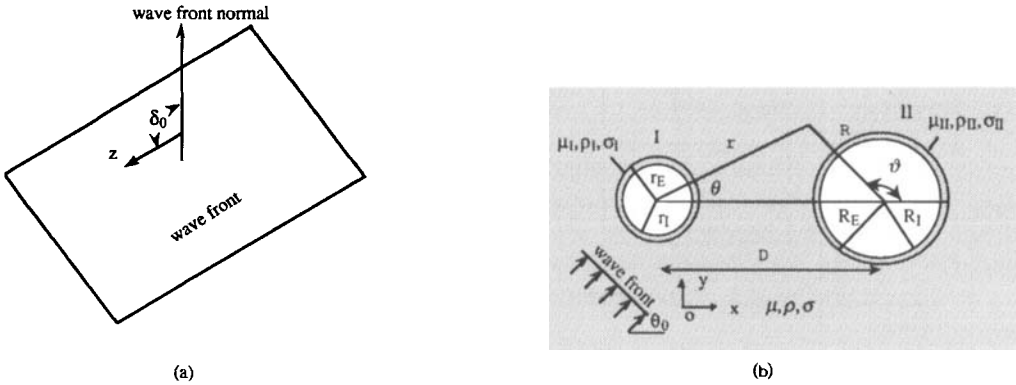

Figure 1. Geometry of the problem

At the interface between the linings and the medium, the continuity and equilibrium conditions will be enforced, e.g.

$$(u_r^{(\mathrm{I,II})}, u_\theta^{(\mathrm{I,II})}, u_z^{(\mathrm{I,II})}) = (u_r, u_\theta, u_z) \tag{5a}$$

$$(\sigma_{rr}^{(\mathrm{I,II})}, \sigma_{r\theta}^{(\mathrm{I,II})}, \sigma_{rz}^{(\mathrm{I,II})}) = (\sigma_{rr}, \sigma_{r\theta}, \sigma_{rz}) \tag{5b}$$

For the problem specified in Figure 1, the wave field consists of the incident seismic waves and the waves scattered by tunnels I and II,

$$\phi = \phi^{\mathrm{i}} + \phi^{\mathrm{I}}(r, \theta, z) + \phi^{\mathrm{II}}(R, \vartheta, z) \tag{6a}$$

$$\varphi = \varphi^{\mathrm{i}} + \varphi^{\mathrm{I}}(r, \theta, z) + \varphi^{\mathrm{II}}(R, \vartheta, z) \tag{6b}$$

$$\chi = \chi^{\mathrm{i}} + \chi^{\mathrm{I}}(r, \theta, z) + \chi^{\mathrm{II}}(R, \vartheta, z) \tag{6c}$$

where superscript i denotes the incident seismic wave.

Co-ordinate system transform

In the numerical analysis, the interaction between the two tunnels is considered by co-ordinate system transformations (Figure 1(b)). The co-ordinate transformations from (r, θ) to (R, ϑ) and from (R, ϑ) to (r, θ) are (see Reference 17)

$$H_n(\alpha_v r)\begin{Bmatrix}\cos n\theta \\ \sin n\theta\end{Bmatrix} = \sum_{m=0}^{\infty} \frac{\varepsilon_m}{2}(H_{n-m}(\alpha_v D) \pm (-1)^m H_{m+n}(\alpha_v D))J_m(\alpha_v R)\begin{pmatrix}\cos m\vartheta \\ \sin m\vartheta\end{pmatrix} \tag{7}$$

and

$$H_n(\alpha_v R)\begin{Bmatrix}\cos n\vartheta \\ \sin n\vartheta\end{Bmatrix} = \sum_{m=0}^{\infty} \frac{\varepsilon_m}{2}(H_{m-n}(\alpha_v D)) \pm (-1)^n H_{m+n}(\alpha_v D))\, J_m(\alpha_v r)\begin{Bmatrix}\cos m\theta \\ \sin m\theta\end{Bmatrix} \tag{8}$$

where

$$\varepsilon_m = \begin{cases} 1, & m = 0 \\ 2, & m = 1,2, \ldots \end{cases} \tag{9}$$

Incident seismic wave

The incident seismic wave can be expressed in terms of potentials. The incident P wave and S wave potentials can be written as[1]

$$\phi^{\mathrm{i}} = \phi_0 \exp(\mathrm{i}k_\alpha \sin\delta_0(x\cos\theta_0 + y\sin\theta_0) + \mathrm{i}k_\alpha z\cos\delta_0 - \mathrm{i}\omega t) \tag{10a}$$

$$\varphi^{\mathrm{i}} = \varphi_0 \exp(\mathrm{i}k_\beta \sin\delta_0(x\cos\theta_0 + y\sin\theta_0) + \mathrm{i}k_\beta z\cos\delta_0 - \mathrm{i}\omega t) \tag{10b}$$

$$\chi^{\mathrm{i}} = \chi_0 \exp(\mathrm{i}k_\beta \sin\delta_0(x\cos\theta_0 + y\sin\theta_0) + \mathrm{i}k_\beta z\cos\delta_0 - \mathrm{i}\omega t) \tag{10c}$$

where δ_0 is the angle of the wave front normal with the z-axis (Figure 1(a)), while θ_0 is the angle that the normal of intersection between the XOY plane and the wave front makes with the x-axis, (Figure 1(b)).

Expressing the wave potentials in polar co-ordinates yields

$$\phi^{\mathrm{i}} = \phi_0 \sum_{m=0}^{\infty} \frac{\varepsilon_m}{2}(\mathrm{i})^m J_m(k_\alpha \sin\delta_0 r)\cos m(\theta - \theta_0)\exp(\mathrm{i}k_\alpha z\cos\delta_0 - \mathrm{i}\omega t) \tag{11a}$$

$$\varphi^{\mathrm{i}} = \varphi_0 \sum_{m=0}^{\infty} \frac{\varepsilon_m}{2}(\mathrm{i})^m J_m(k_\beta \sin\delta_0 r)\cos m(\theta - \theta_0)\exp(\mathrm{i}k_\beta z\cos\delta_0 - \mathrm{i}\omega t) \tag{11b}$$

$$\chi^{\mathrm{i}} = \chi_0 \sum_{m=0}^{\infty} \frac{\varepsilon_m}{2}(\mathrm{i})^m J_m(k_\beta \sin\delta_0 r)\cos m(\theta - \theta_0)\exp(\mathrm{i}k_\beta z\cos\delta_0 - \mathrm{i}\omega t) \tag{11c}$$

where J_m is a Bessel function of the first kind. The displacement and stress due to the incident waves can be determined using the expressions given elsewhere.[1]

Method of successive reflections

The method of successive reflections is applied to decouple the responses of the two tunnels so that the solution for each tunnel can be determined independently. This approach was first proposed by Thiruvenkatachar and Viswanathan,[15] who studied the response of a loaded cylinder in a half-plane using co-ordinate transforms between the cylindrical co-ordinate system and Cartesian co-ordinates. Scheidl and Ziegler[16] used the method to investigate the interaction between Rayleigh waves and a rigid inclusion buried in a half-plane.

The solution procedure is as follows:

(1) The waves in the lining and the outgoing wave in the medium are determined at tunnel I using the boundary conditions. The incoming wave from tunnel II is assumed to be zero.
(2) The waves in the lining and the outgoing wave in the medium at tunnel II are obtained from the boundary conditions. The incoming wave from tunnel I is then included using the coordinate transform of the outgoing wave at tunnel I.
(3) The waves in the lining and the outgoing wave in the medium at tunnel I are reevaluated with the incoming wave from tunnel II included.
(4) Steps 2 and 3 are repeated until the solution converges, where at each step, the waves in the lining and the outgoing wave in the medium are determined using the boundary conditions and the incoming wave from the other tunnel calculated during the previous step.

Convergence

The convergence of the method of successive reflections was discussed by Thiruvenkatachar and Viswanathan[10] for the wave scattering by a cylinder in a half-space. The convergence of the method is now examined for the specific case of two unlined cavities. Without loss of generality, attention is focused on the response of cavity I as a result of the incident wave boundary conditions and the wave reflection between the two cavities.

We begin by approximating the Bessel functions by the asymptotic forms for the long wavelength, i.e. $\alpha_v D \ll 1$ (this is reasonable given $z^2/4 \ll n$, $\mathrm{Re}\, z > 0$ and $n > 0$, Watson[17]).

$$J_n(z) \approx \frac{(z/2)^n}{n!} \tag{12a}$$

$$H_n(z) \approx -\mathrm{i}\left(\frac{2}{z}\right)^n \frac{(n-1)!}{\pi} \tag{12b}$$

where H_n is the Hankel function of the first kind.

Therefore, with the incoming wave from cavity II excluded, a constant k_1 can be found for the upper bound of the outgoing wave coefficients due to unit incident waves

$$(|A_n^{\mathrm{I}}|, |B_n^{\mathrm{I}}|, |C_n^{\mathrm{I}}|, |D_n^{\mathrm{I}}|, |E_n^{\mathrm{I}}|, |F_n^{\mathrm{I}}|) < k_1 \frac{(r;\ \alpha/2)^{2n}}{n!(n-1)!} \quad (n = 0,1,2, \ldots) \tag{13}$$

where α = maximum of ($|\alpha_{\mathrm{L}}|$ and $|\alpha_{\mathrm{T}}|$).

Substituting equation (13) into equation (7) and using equation (12), it is then possible to find a positive number k_D so that the following inequality holds for the incoming wave coefficients for cavity II:

$$(|a_m^{\mathrm{II}}|, |b_m^{\mathrm{II}}|, |c_m^{\mathrm{II}}|, |d_m^{\mathrm{II}}|, |e_m^{\mathrm{II}}|, |f_m^{\mathrm{II}}|) < k_1 k_D \sum_{k=0}^{\infty} \varepsilon_m \frac{(r;\alpha/2)^{2k}(m+k-1)!}{(D\alpha/2)^{(m+k)} k!(k-1)!} \tag{14}$$

Similarly, the coefficients of the outgoing wave of cavity II are bounded as follows:

$$(|A_m^{II}|, |B_m^{II}|, |C_m^{II}|, |D_m^{II}|, |E_m^{II}|, |F_m^{II}|) < k_I k_D k_{II} \sum_{k=0}^{\infty} \varepsilon_m \frac{(r_i R_i \alpha^2/4)^{2(k+m)}(m+k-1)!}{(D\alpha/2)^{(m+k)} k!\,(k-1)!m!(m-1)!} \tag{15}$$

The incoming wave for cavity I can be obtained from the outgoing wave from cavity II using the co-ordinate transform once more

$$(|a_n^I|, |b_n^I|, |c_n^I|, |d_n^I|, |e_n^I|, |f_n^I|) < k_I k_D^2 k_{II} \sum_{m=0}^{\infty} \varepsilon_n \sum_{k=0}^{\infty} \varepsilon_m \frac{(r_i R_i \alpha^2/4)^{2(k+m)}(m+k-1)!(m+n-1)!}{(D\alpha/2)^{(2m+k+n)} k!\,(k-1)!m!(m-1)!} \tag{16}$$

It can be proved that the series defined by

$$k_D^n = k_D^2 \sum_{k=0}^{\infty} \varepsilon_n \sum_{k=0}^{\infty} \varepsilon_m \frac{(r_i R_i \alpha^2/4)^{2(k+m)}(m+k-1)!(m+n-1)!}{(D\alpha/2)^{(2m+k+n)} k!\,(k-1)!m!(m-1)!} \tag{17}$$

is uniformly convergent for a given n. Hence, the outgoing wave for cavity I (with incoming wave from cavity II included) is subject to

$$(|A_n^I|, |B_n^I|, |C_n^I|, |D_n^I|, |E_n^I|, |F_n^I|) < k_I (1 + k_I k_D^n k_{II}) \frac{(r_i \alpha/2)^{2n}}{n!(n-1)!} \tag{18}$$

Following m iterations of the method of successive reflections, the outgoing wave of cavity I gives

$$(|A_n^I|, |B_n^I|, |C_n^I|, |D_n^I|, |E_n^I|, |F_n^I|) < \sum_{j=0}^{m} k_I (k_I k_D^n k_{II})^j \frac{(r_i \alpha/2)^{2n}}{n!(n-1)!} = k_I \frac{1 - (k_I k_D^n k_{II})^{m+1}}{1 - k_I k_D^n k_{II}} \frac{(r_i \alpha/2)^{2n}}{n!(n-1)!} \tag{19}$$

The method of successive reflections therefore converges provided $k_I k_D^n k_{II} < 1$.

It is difficult to convert equation (19) into an explicit convergence criterion defined in terms of tunnel spacing D and wavelength. However, the spacing D between the two cavities in equation (17) can be changed for a given r_i and R_i so that $k_I k_D^n k_{II} < 1$. The procedure therefore converges when the wavelength is long enough or there is a sufficiently large spacing between the two cavities. The $k_I k_D^n k_{II}$ values for the dominant terms (e.g. $n = 2$) are particularly small ($k_I k_D^n k_{II} \ll 1$), so that convergence is rapid. In addition, for any specific problem where convergence is of particular concern, the efficiency of the technique permits a large number of iterations so that any possible divergence can be revealed.

The convergence and accuracy of the MSR has also been validated by analysing the response of twin tunnels in a half-space subjected to horizontally polarized shear waves. For SH waves, the half-space can be treated as a line of symmetry in the manner of Balendra *et al.*,[8] whose results are used for comparison. By considering the interaction of four tunnels, the results for two tunnels close to the half-space boundary are evaluated.

Figure 2 shows solutions for tunnels at normalized burial depth to the tunnel axes $H/r_e = 2{\cdot}5$. Tunnels located at a considerable distance ($D/r_e = \infty$) and close together ($D/r_e = 5$) have been examined where the normalized frequency $a_0 = \omega r_i/v_T = 0{\cdot}77$ and the tunnel linings have modulus $\mu/\mu_m = 76$ times that of the surrounding medium. A good agreement is obtained between the two solution procedures.

NUMERICAL STUDY

Geometry

The response of the twin lined tunnels to seismic ground motion is clearly a function of a considerable number of geometrical and material properties. In order to simplify this study, the response will be examined for tunnels of equal radius ($r_i = R_i$) and with identical linings ($r_e = R_e$, $\mu = \mu_I = \mu_{II}$). The Poisson ratio for the medium and liners are 0·25 and 0·3, respectively. Furthermore, the centre to centre spacing of the tunnels will be taken as $D = 3{\cdot}25r_i$, $4{\cdot}25r_i$ or ∞, the liner thickness $r_e - r_i = r_i/8$ and the incident seismic waves examined will be parallel to either the YOZ plane ($\theta_0 = \pi/2$) or XOZ plane ($\theta_0 = 0$). The two tunnels have axes parallel

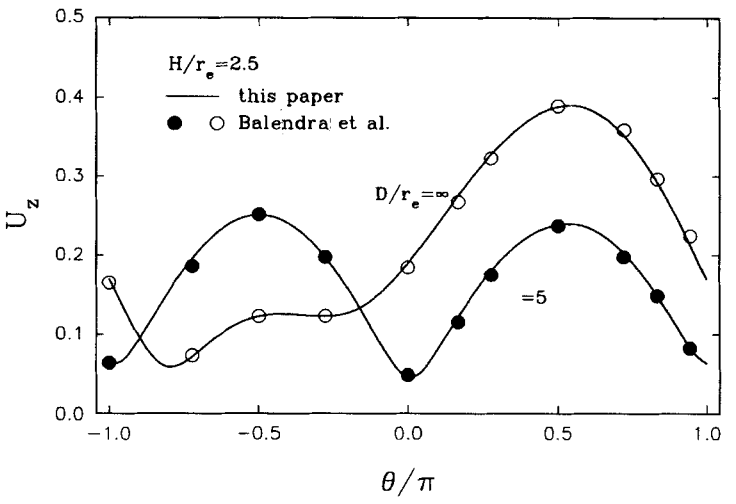

Figure 2. Comparisons of the solutions by the authors and those (symbols) by Balendra *et al.* ($H/r_e = 1{\cdot}5, r_e/r_i = 1{\cdot}2, a_0 = 0{\cdot}64, \theta_0 = \pi/6$ and $\delta_0\pi/2$)

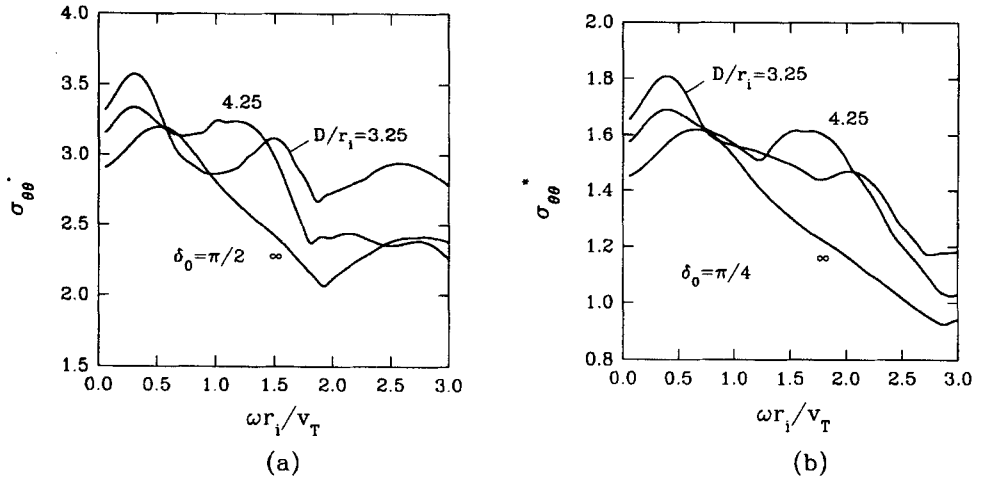

Figure 3. Maximum stress response versus normalized frequency; response to incident S waves at the inside surface of the liner and position $z = 0$ ($\theta_0 = \pi/2$, $\mu/\mu_m = 3$)

to z, so that for $\theta_0 = \pi/2$ the tunnels have symmetric response about the YOZ plane and only one tunnel response needs to be reported. Alternatively, for $\theta_0 = 0$ the tunnel responses are different but symmetric about the horizontal diameters. For all the results presented, the displacements and stresses are normalized by k_β and μk_β^2, respectively.

Incident S wave — interaction between the tunnels

To examine the interaction of the two tunnels, Figure 3 shows predictions of normalized hoop stress for tunnels at three different spacings $D/r_i = 3{\cdot}25, 4{\cdot}25$ and ∞ and for two different incident angles $\delta_0 = \pi/2$ and $\pi/4$. To determine the effect of the frequency of the seismic ground motion, a range of normalized vibration frequencies $a_0 = \omega r_i/v_T$ is considered. The results in Figure 2 reveal that the through-soil interaction between

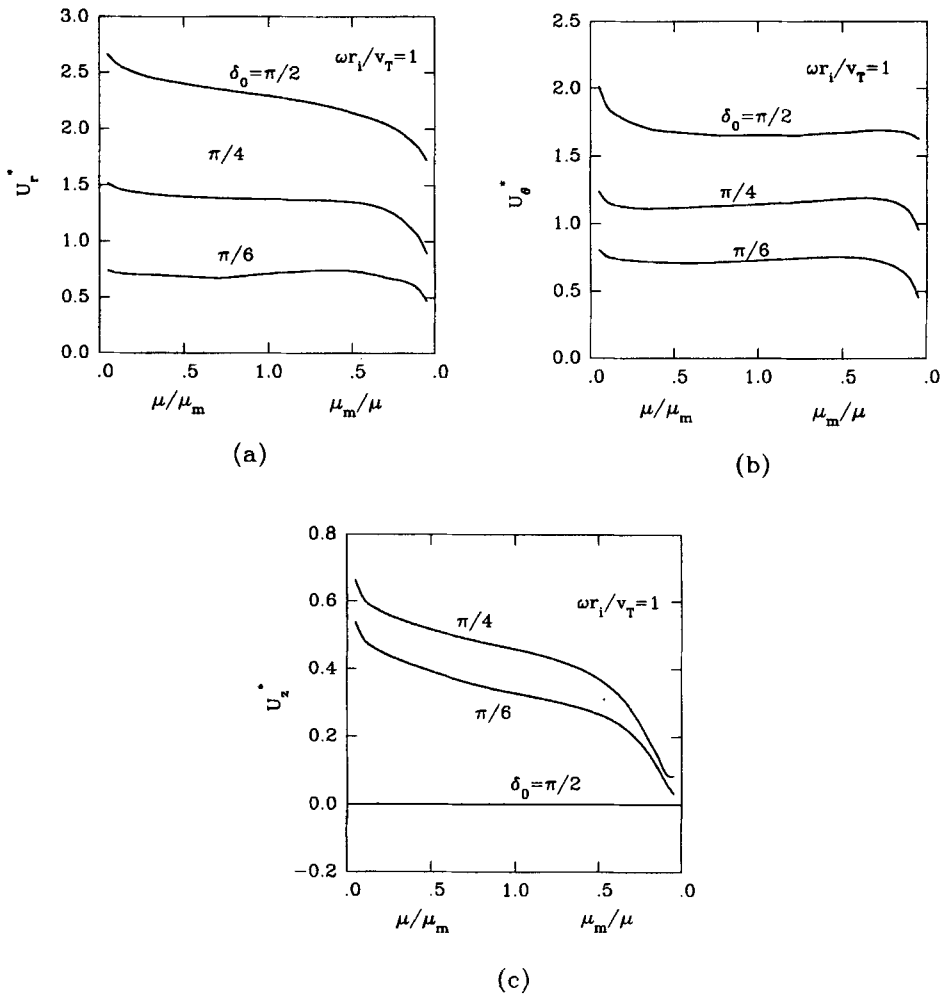

Figure 4. Maximum displacement response versus normalized frequency; response to incident S waves at the outside surface of the liner and position $z = 0$ ($\theta_0 = 0$, $D/r_i = 3{\cdot}25$)

the closely spaced tunnels is significant, and the effect is frequency dependent. For most frequencies, reductions in the tunnel to tunnel spacings leads to greater hoop stresses in the tunnel lining.

At low vibration frequency $a_0 < 0{\cdot}5$, the tunnel to tunnel interaction for all three tunnel spacings is insignificant. As normalized frequency a_0 increases, however, tunnel response becomes significantly influenced by spacing. For $0{\cdot}5 < a_0 < 2{\cdot}5$, the hoop stress $\sigma^*_{\theta\theta}$ is up to 30% less for an isolated tunnel $D/r_i = \infty$ than for $D/r_i = 3{\cdot}25$ or $4{\cdot}25$. For tunnels with $D < 3r_i$, the increase in hoop stress due to through-soil interaction is expected to be even more important.

Incident S wave – influence of lining modulus

To examine the influence of lining design, Figures 4 and 5 show solutions for maximum normalized displacements U_r^*, U_θ^* and U_z^*, and stresses $\sigma^*_{\theta\theta}$, σ^*_{zz} and $\sigma^*_{z\theta}$ for the specific normalized frequency $a_0 = 1$, for a range of modular ratios μ/μ_m and for three different incident angles δ_0.

The normalized radial and circumferential displacements are the greatest responses under plane strain conditions, $\delta_0 = \pi/2$. They peak at low modulus ratio μ/μ_m, but remain nearly constant when the modular

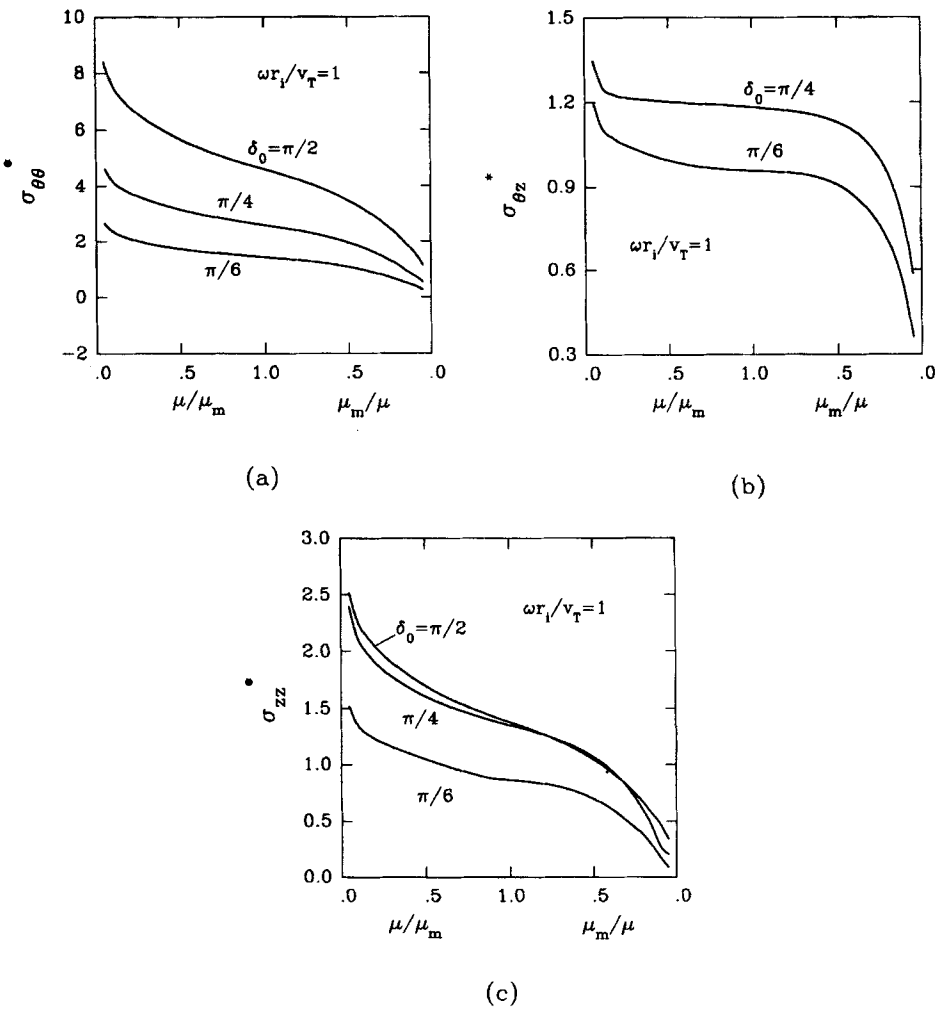

Figure 5. Maximum stress response versus normalized frequency; response to incident S waves at the inside surface of the liner and position $z = 0$ ($\theta_0 = 0$, $D/r_i = 3{\cdot}25$)

ratio μ/μ_m ranges from 0·25 to 4. Normalized longitudinal displacement also decreases monotonically as μ/μ_m increases, but is generally more sensitive to any changes in the modular ratio.

Normalized stress amplitudes $\sigma^*_{\theta\theta}$, σ^*_{zz} and $\sigma^*_{z\theta}$ at the inner surface of the lining all steadily decrease as the surrounding modulus μ_m decreases relative to that of liners μ. All values tend towards zero as modular ratio μ_m/μ approaces zero. As noted for the normalized displacement, the two-dimensional loading condition $\delta_0 = \pi/2$ induces the greatest stress. Circumferential stresses $\sigma^*_{\theta\theta}$ are largest in magnitude.

Incident S wave — influence of incident angle θ_0

The behaviour of the two tunnels is now examined under plane strain condition ($\delta_0 = \pi/2$) with incident angles $\theta_0 = 0$, $\pi/4$ and $\pi/2$ and a range of vibration frequencies. The tunnels are spaced at distance $D/r_i = 3{\cdot}25$ and have lining modulus three times that of the ground medium ($\mu/\mu_m = 3$). Figures 6(a) and 6(b) show the amplitude of the normalized stress $\sigma^*_{\theta\theta}$ for tunnel I and tunnel II, respectively.

For an isolated tunnel, the response is independent of the incident angle θ_0. However, for these closely spaced tunnels, the response is significantly affected by the orientation of the incoming wave. Firstly, Figures 6(a) and 6(b) clearly show that the effect of the incident angle θ_0 is frequency dependent. Circumferential

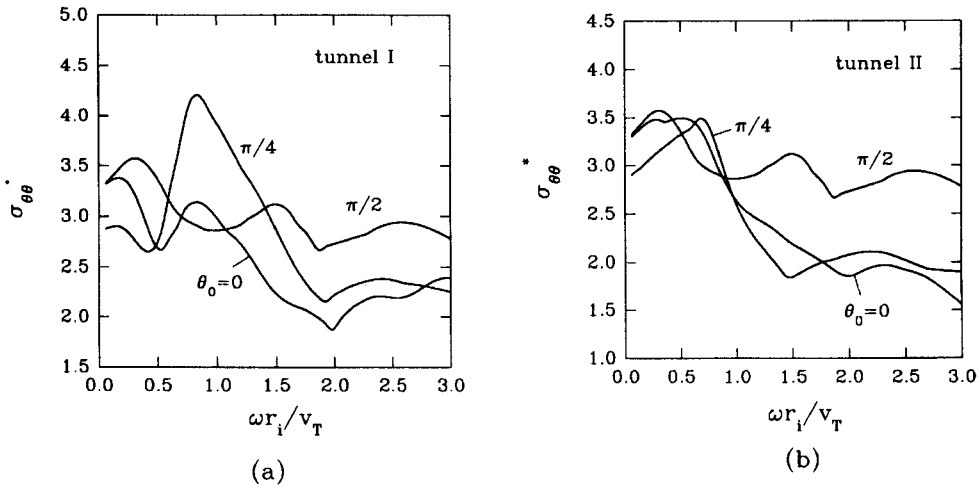

Figure 6. Maximum stress response versus normalized frequency; response to incident S waves at the inside surface of the liner and position $z = 0$ ($\delta_0 = \pi/2$, $\mu/\mu_m = 3$)

stress $\sigma^*_{\theta\theta}$ for tunnel I has the greatest amplitude when $\theta_0 = \pi/4$ and at the normalized frequency $a_0 = 0{\cdot}8$. For larger values of normalized frequency, $a_0 > 1{\cdot}5$, the responses are less frequency dependent and the vertically moving seismic wave ($\theta_0 = \pi/2$) induces the highest hoop stresses in both tunnels. For tunnel II, the peak stress occurs when $0{\cdot}2 < a_0 < 0{\cdot}8$, but is not quite as great and is less dependent on θ_0.

Incident P wave

The effect of lining modulus μ/μ_m on the tunnel response to longitudinal seismic waves has also been evaluated (Figures 7 and 8). Figure 7 shows normalized radial, circumferential and longitudinal displacements for $\theta_0 = \pi/2$, for three incident wave angles δ_0, and a range of the modular ratios. The trends are similar to those observed earlier for tunnel response to shear waves, but with stress and displacement amplitudes somewhat smaller. The response increases as the modular ratio increases. As before, the two-dimensional solution provides a conservative estimate of the three-dimensional response. Compared to the response of the incident S wave, the scattering of the incident P wave around the tunnels only amplifies the incident seismic wave slightly (20 per cent) in the range of frequency studied.

The amplitudes of normalized liner stress are plotted in Figure 8. Compared to the normalized displacement amplitudes, the stresses are more sensitive to changes in the modular ratio. Trends are similar to those seen in Figure 5 for response to shear waves.

Incident P wave-interaction between the tunnels

The interaction between the tunnels is shown in Figure 9 for different angles $\delta_0 = \pi/2$ and $\pi/4$. Unlike the prediction made for tunnel response to an S wave, the hoop stress $\sigma^*_{\theta\theta}$ decreases rapidly as the frequency is increased. The through-soil interaction between the tunnels is not as significant as it is for an incident S wave. At most frequencies, the stress predictions for the closely spaced tunnels are higher than those for an isolated tunnel, though the difference is not very significant.

Incident P wave-influence of incident angle

Figure 10 shows the hoop stress response of the two tunnels. The peak hoop stress is produced for an incident angle $\delta_0 = 0$ and a normalized frequency $a_0 = 1$. However, less response is induced in tunnel II for incident angle $\theta_0 = 0$ since it is shielded by tunnel I (tunnel II is in the 'shadow' of tunnel I).

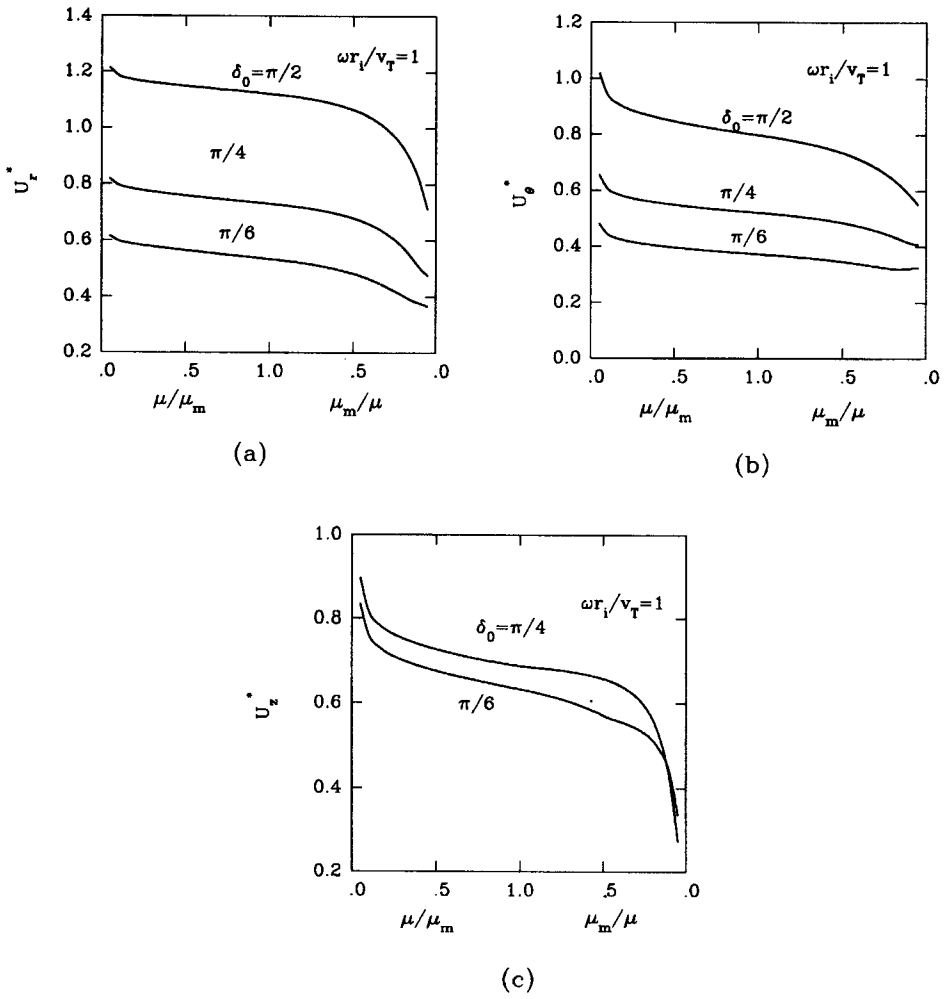

Figure 7. Maximum displacement response versus normalized frequency; response to incident P waves at the outside surface of the liner and position $z = 0$ ($\theta_0 = \pi/2$, $D/r_i = 3{\cdot}25$)

Shallow buried tunnels

The primary focus of the present work is the analysis of the three-dimensional response of twin deeply buried tunnels. To complete the study, however, the influence of the ground surface (half-space boundary) on shallow buried tunnels is briefly examined. This serves to demonstrate how the model can be used to examine this particular problem involving twin shallow buried tunnels, and comparisons with full-space solutions illustrate under what circumstances the half-space boundary may be important.

Figure 11 contains results obtained using three lining conditions, with a direct comparison of the half-space and full space results. Solutions are for normalized depth to the tunnel axes $H/r_e = 2{\cdot}5$ for two different modular ratios ($\mu/\mu_m = 4$ and 20), and two different density ratios $\rho/\rho_m = 1$ and 3. The axis to axis distance between the tunnels is $D/r_e = 5$. Distributions of normalized displacement U_z are given for the full tunnel circumference.

Solutions for the half-space are obtained using the symmetry condition discussed earlier with respect to the work of Balendra *et al.*[8] (response to SH wave is evaluated using wave scattering associated with four tunnels). The 'full-space' solutions are obtained by considering wave reflection from two tunnels. The input ground motion introduced to those structures are half-space wave functions,[8] however, where the effect of the 'half-space' boundary on the incident wave is included. Therefore, the differences between the 'full-space' and

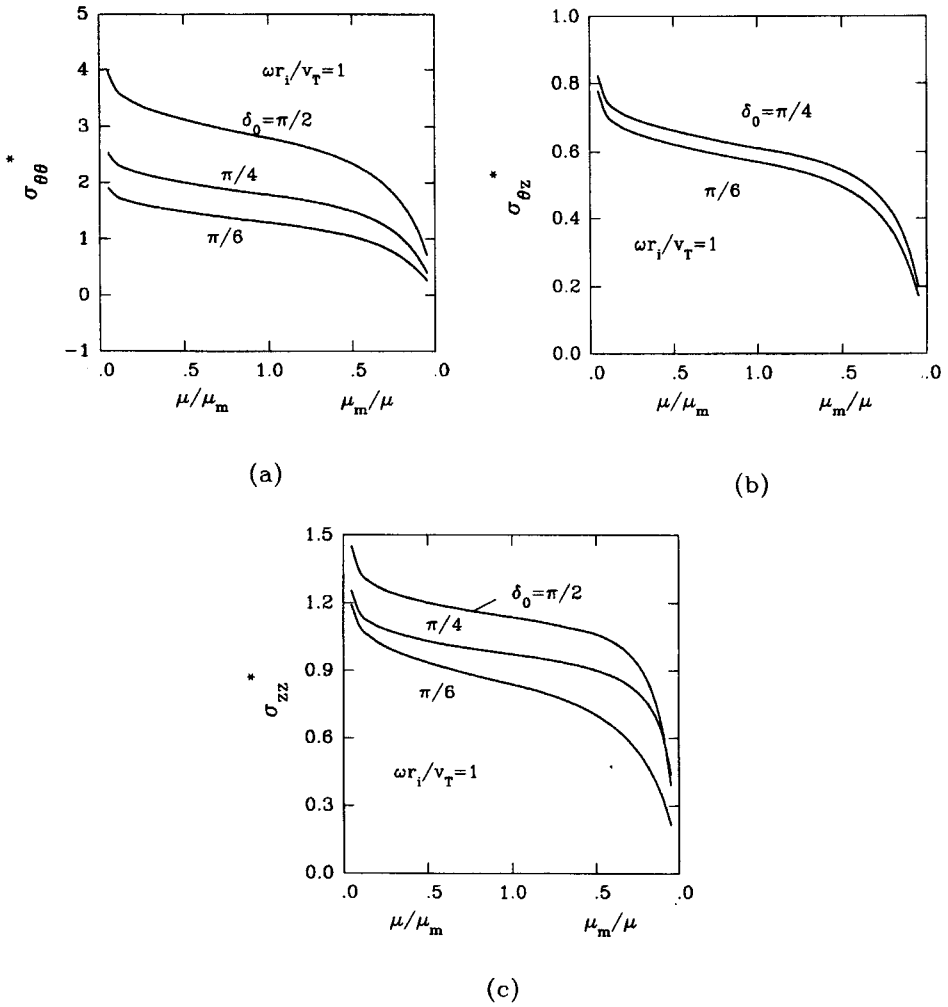

Figure 8. Maximum stress response versus normalized frequency; response to incident P waves at the inside surface of the liner and position $z = 0$ ($\theta_0 = \pi/2$, $D/r_i = 3{\cdot}25$)

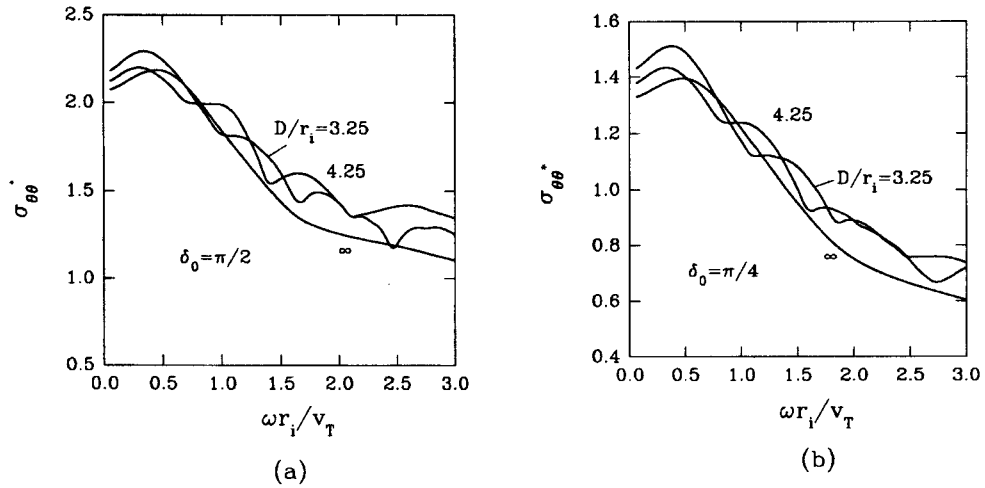

Figure 9. Maximum stress response versus normalized frequency; response to incident P waves at the inside surface of the liner and position $z = 0$ ($\theta_0 = \pi/2$, $\mu/\mu_m = 3$)

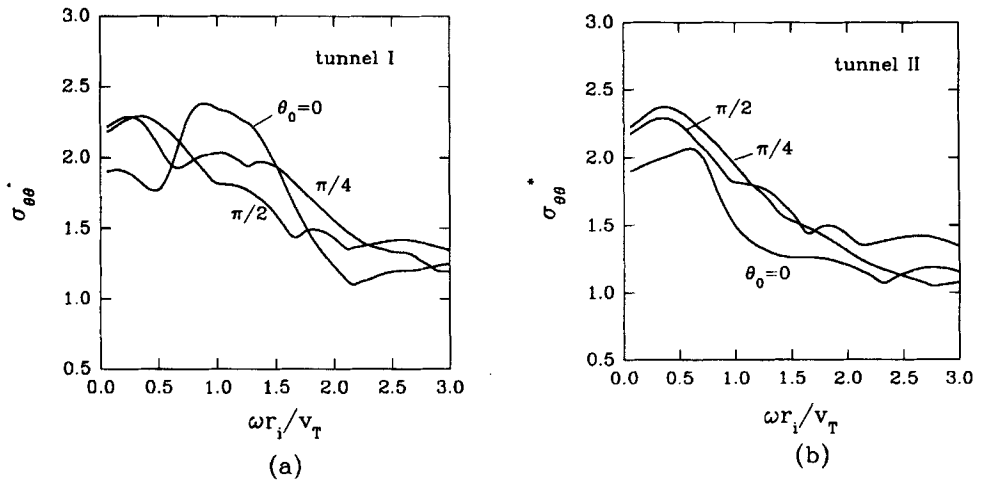

Figure 10. Maximum stress response versus normalized frequency; response to incident P waves at the inside surface of the liner and position $z = 0$ ($\delta_0 = \pi/2$, $\mu/\mu_m = 3$ and $D/r_i = 3{\cdot}25$)

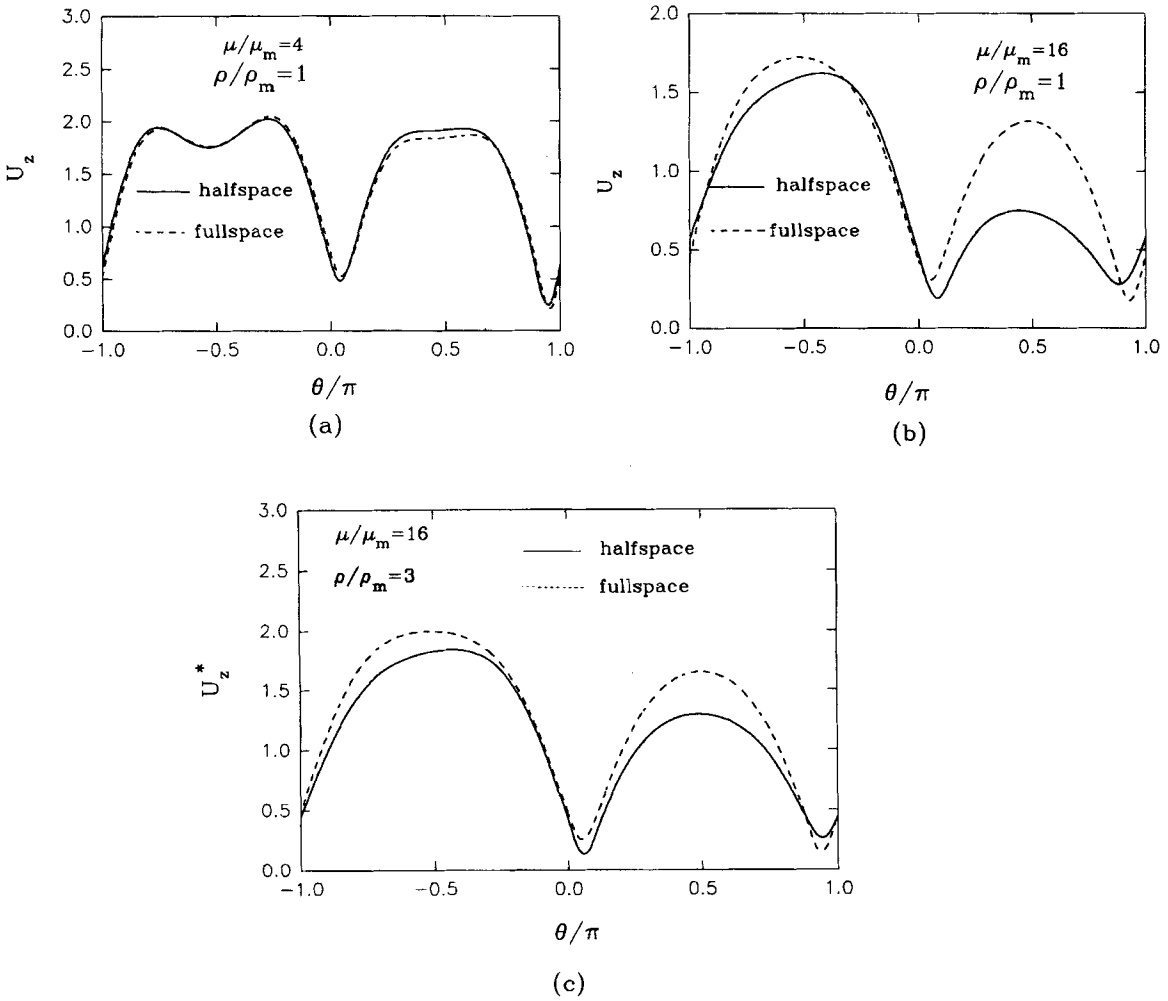

Figure 11. Influence of the free surface on the response of the twin tunnels ($\delta_0 = \pi/2$, $a = 1{\cdot}2$, $H/r_e = 1{\cdot}5$, and $D/r_e = 5$)

'half-space' solutions are the result of wave reflection (interaction) between each tunnel and the horizontal stress-free boundary.

The differences between the half-space and full-space solutions given in Figures 11(a) and 11(c) are noticeable, but not great. In these cases, the tunnel-half-space interaction is having only a small effect on the dynamic response. Where both the lining modulus and the lining density are high, however, (Figure 11(b) interaction between the tunnel crown and the free surface becomes significant. These and other results not reported here, reveal that it is reasonable to use the method of successive reflections to obtain predictions for the seismic response of a pair of tunnels located at least one tunnel diameter from a half-space boundary (input ground motion must include the effect of the free surface and either modular ratio or density ratio must be low).

CONCLUSIONS

In this study, the dynamic response of twin tunnels due to seismic waves is evaluated by applying the method of successive reflections. The uncoupled tunnel responses are solved independently and the interaction between them is taken into account using wave expansions and co-ordinate transformations. Numerical results showed that interaction between tunnels may be important, and that the two-dimensional responses and three-dimensional responses are quite different. The plane strain condition is generally conservative. Lower normalised stresses are predicted in the linings when the soil modulus is low. It is also found that the response depends on the spacing between the tunnels, the incident angle of the seismic wave and the ratio of tunnel liner modulus to that of the surrounding soil. A two-dimensional study of twin shallow buried structures revealed that under certain circumstances, the tunnel-half-space interaction does not appear to be important where depth of burial is at least one tunnel diameter. The method of successive reflections described in this work can then be used to predict tunnel response, provided the incident wave is modified to include the effect of the half-space.

ACKNOWLEDGEMENTS

Support for this work has been provided through research and equipment grants to the first author from the Natural Sciences and Engineering Research Council of Canada.

REFERENCES

1. H. Y. Pao and C. C. Mow, *The Diffraction of Elastic Waves and Dynamic Stress Concentrations*, Crane-Russak, New York, 1973.
2. M. D. Trifunac, 'Scattering of plane SH waves by a semi-cylindrical canyon', *Earthquake eng. struct. dyn.* **1**, 267–281. (1973).
3. H. L. Wong and M. D. Trifunac, 'Scattering of plane SH waves by a semi-elliptical canyon', *Earthquake eng. struct. dyn.* **3**, 157–169. (1974).
4. H. L. Wong and P. C. Jennings, 'Effect of canyon topography on strong ground motion', *Bull. seism. soc. Am.* **65**, 1239–1257 (1975).
5. M. Dravinski, 'Scattering of SH waves by subsurface topography', *J. eng. mech. div. ASCE* **108**, 1–17 (1982).
7. V. W. Lee and M. D. Trifunac, 'Response of tunnels to incident SH-waves', *J. eng. mech. div. ASCE* **105**, 643–659 (1979).
8. T. Balendra, D. P. Thambiratnam, C. G. Koh and S. L. Lee, 'Dynamic response of twin circular tunnels due to incident SH-waves', *Earthquake eng. struct. dyn.* **12**, 181–201 (1984).
9. T. Okumura, N. Takewaki and K. Shimizu, 'Dynamic response of twin circular tunnels during earthquakes', *Proc. 4th U.S.–Japan workshop on earthquake disaster prevention for lifeline systems*, Los Angeles, CA, 1992, pp. 181–191.
10. K. C. Wong, A. H. Shah and S. K. Datta, 'Diffraction of elastic waves in a half-space, II. Analytical and numerical solutions', *Bull. seism. soc. Am.* **75**, 69–92 (1985).
11. A. H. Shah, K. C. Wong and S. K. Datta, 'Single and multiple scattering of elastic waves in two dimensions', *J. accoust. soc. Am.* **74**, 1033–1043 (1983).
12. Y. F. Chin, R. K. N. D. Rajapakse and S. K. Datta, 'Dynamics of buried pipes in back-filled trench', *Soil dyn. earthquake eng.* **6**, 158–163 (1987).
13. S. W. Liu, S. K. Datta, K. R. Khair and A. H. Shah, 'Dynamic response of pipelines buried in back-filled trenches', *J. pressure vessel technol. ASME* **113**, 429–436 (1991).
14. F. Guan and I. D. Moore, 'Three dimensional dynamic response of twin cavities due to travelling loads', *J. eng. mech. ASCE* **120**, 637–653 (1994).
15. V. R. Thiruvenkatachar and K. Viswanathan, 'Dynamic response of an elastic half-space with cylindrical cavity to time-dependent surface tractions over the boundary of the cavity', *J. math. appl. mech.* **14**, 541–567 (1965).
16. W. Scheidl and F. Ziegler, 'Interaction of a pulsed Rayleigh surface wave and a rigid cylindrical inclusion', in J. Miklowitz and J. D. Achenbach (eds) *Modern Problems in Elastic Wave Propagation*, Wiley, New York, 1978, pp. 145–169.
17. G. N. Watson, *A Treatise of the Theory of Bessel Functions*, Cambridge Univ. Press, London and New York, 1957.